High spin states in ^{143}Sm

R. Raut, S. Ganguly, R. Kshetri, P. Banerjee, S. Bhattacharya, B. Dasmahapatra, A. Mukherjee, G. Mukherjee, M. Saha Sarkar, and A. Goswami
Saha Institute of Nuclear Physics 1/AF Bidhannagar, Kolkata-700064, India

G. Gangopadhyay
Department of Physics, University of Calcutta 92, A.P.C Rd. Kolkata-700009, India

S. Mukhopadhyay, Krishichayan, A. Chakraborty, and S. S. Ghughre
UGC-DAE Consortium for Scientific Research LB-8, Sector III, Bidhannagar, Kolkata-700098, India

T. Bhattacharjee and S. K. Basu
Variable Energy Cyclotron Center 1/AF Bidhannagar, Kolkata-700064, India
(Received 6 October 2005; published 11 April 2006)

The high spin states of ^{143}Sm have been studied by in-beam γ-spectroscopy following the reaction ^{130}Te(^{20}Ne,7n)^{143}Sm at $E_{\rm lab} = 137$ MeV, using a Clover detector array. More than 50 new gamma transitions have been placed above the previously known $J^{\pi} = 23/2^{-}$, 30 ms isomer at 2795 keV. The level scheme of ^{143}Sm has been extended up to 12 MeV and spin-parity assignments have been made to most of the newly proposed level. Theoretical calculation with the relativistic mean field approach using blocked BCS method, has been performed. A sequence of levels connected by $M1$ transitions have been observed at an excitation energy $\sim$8.6 MeV. The sequence appears to be a magnetic rotational band from systematics.

DOI: 10.1103/PhysRevC.73.044305 PACS number(s): 27.60.+j, 23.20.Lv, 23.20.En

I. INTRODUCTION

Generation of angular momentum for weakly deformed nuclei in the vicinity of the ^{146}Gd core has been the subject of great interest in recent years. These nuclei, at low excitation energies, show complex and irregular pattern, as expected of nuclei near shell closure and are dominated by single and multiparticle excitations. However, at higher excitation energies and angular momenta, the same nuclei have been observed to exhibit vast vistas of excitation phenomena. It can be cited that, shape evolution from spherical to prolate, oblate or triaxial, has been observed in this region. Superdeformed bands have also been established in ^{142,145}Sm [1,2] and bands of triaxial origin have been found in ^{138,139}Nd [3]. Moreover, due to the availability of particles and holes in the high j-orbital, such as $\pi h^{n}_{11/2}$ and $\nu h^{-n}_{11/2}$, phenomena like magnetic rotation could be expected. For instance, dipole bands have been observed in ^{139}Sm [4], $^{143-146}$Tb [5–8], ^{142,144}Gd [9,10] and ^{137}Nd [11]. Among the dipole bands observed in this region, those in ^{139}Sm [1], ^{143}Tb [5], and ^{142}Gd [12], have been interpreted as magnetic rotational band in the light of TAC calculations [14] and lifetime measurements. The phenomenon of magnetic rotation has been a subject of zealous pursuit since the last decade, after it's maiden observation in the light mass Pb isotopes [13]. Such interest stems out from the novelty of the process in generating angular momentum in nuclei with very small deformation and low quadrupole collectivity.

The nucleus ^{143}Sm ($Z = 62$) was studied earlier using the reaction ^{126}Te(^{22}Ne,5n), ^{128}Te (^{22}Ne,7n), ^{130}Te(^{20}Ne,7n) [15] and also by ^{142}Nd(α, 3n) [16]. Kowanacki *et al.* [16] performed in-beam experiment using the α beam and two detector coincidence set up and proposed a level scheme of ^{143}Sm up to spin 29/2$\hbar$ at an excitation energy of 4369 keV. In both these experiments [15,16], a 30 ms isomer was observed at 2795 keV, with a spin of 23/2^{-}. The observed level structure was theoretically interpreted [16] as the coupling of the $h_{11/2}$ neutron hole to the doubly even ^{144}Sm core excitations. The coupling of the first 2^{+} and 3^{-} state of the ^{144}Sm core to a neutron hole is treated in terms of the weak and intermediate coupling models. The results obtained in these calculations were in reasonably good agreement with the experimental data. The energies of the three quasiparticle states, resulting from the coupling of the h$_{11/2}$ neutron hole to the two proton excitation in the core were also reproduced in the calculations.

The present work was initiated with the motivation to extend the level scheme to higher spin states of ^{143}Sm, since the level scheme by Kowanacki *et al.* [16] is largely unchartered in the energy realm expected to be dominated by the single and multiparticle excitations. This work also intended to look for any possible occurence of magnetic rotation in this nucleus, since it has very small deformation and low quadrupole collectivity, and there are $\nu h_{11/2}$ hole and proton particle excitation to $\pi h_{11/2}$ at higher angular momentum.

II. EXPERIMENT

In the present experiment, the high spin states of ^{143}Sm were populated by the reaction ^{130}Te(^{20}Ne,7n) at a beam energy of $E_{\rm lab} = 137$ MeV. The ^{20}Ne beam was obtained from the Variable Energy Cyclotron Center (VECC), Kolkata. The target was $\sim$5 mg/cm^2 ^{130}Te (99% enriched) with $\sim$2mg/cm^2

 ©2006 The American Physical Society

alumunium backing. The detector system used was the Indian National Gamma Array (INGA), stationed at VECC, Kolkata. For this experiment, the INGA comprised of six Compton suppressed Clover detectors, two each at angles 40°, 90°, and 125°, with respect to the beam direction. Four of these detectors (at $\theta = 40°$ and 125°) were in the median plane, and the remaining two (at $\theta = 90°$) at $\phi = 36°$, out of plane. This geometry allows the polarization measurement of the gamma rays. About 5×10^8, two- and higher fold events were recorded in the present experiment.

III. ANALYSIS

The coincidence events were sorted into

(i) a symmetric γ-γ matrix with a time gate of 100 ns which was used to generate various background subtracted gated spectra.

(ii) an asymmetric (angle dependent) γ-γ matrix to determine the $R_{\rm DCO}$ ratios, defined as

$$R_{\rm DCO} = \frac{I_{\gamma_1}[\text{observed at } 90°, \text{ gated by } \gamma_2 \text{ at } 40°]}{I_{\gamma_1}[\text{observed at } 40°, \text{ gated by } \gamma_2 \text{ at } 90°]}$$

which were compared with the theoretical $R_{\rm DCO}$ ratios for spin assignments. The theoretical ratios were calculated by using the code ANGCOR [17]. Theoretically, as far as the present set-up is concerned, gate on a pure dipole transition, renders a DCO ratio of 1.65 for pure quadrupole transition, 1.00 for pure dipole transition, greater than 1.0 for mixed (mixing ratio, δ greater than 0) and less than 1.0 (δ less than 0) transition.

(iii) two matrices to deduce the electromagnetic character of the gamma transitions, by determining the polarization directional correlation orientation (PDCO) ratio [18]. The asymmetry of the Compton scattered polarized photons are obtained from

$$\text{PDCO} = \frac{a(E_\gamma)N_\perp - N_\parallel}{a(E_\gamma)N_\perp + N_\parallel},$$

where $N_\perp$ and $N_\parallel$ represent the number of γ-rays with scattering perpendicular and parallel to the emission plane and a is the correction term due to the asymmetry of the present experimental configuration. It is defined as

$$a = \frac{N_\parallel(\text{unpolarized})}{N_\perp(\text{unpolarized})}.$$

For the present setup, the energy dependence of the correction term was determined with an ^{152}Eu source. Figure 1 shows the variation of a with $E\gamma$ and it was fitted with the expression $a(E_\gamma) = a_0 + a_1 E_\gamma$ resulting into $a_0 = 1.03$ and $a_1 \sim 10^{-5}$, where E_γ is in keV.

The experimental asymmetry, PDCO, for the transitions of interest was evaluated from two γ-γ matrices. One matrix contained events in which one of the γ-rays was scattered inside the clover, at 90°, in the direction perpendicular to the emission plane (those events were put on y-axis) while a coincident γ-ray was registered in any clover at angles 40° and 125° (those events were put on x-axis). The other matrix was almost similar, except for the fact that the γ-rays scattered inside the clover, at 90°, in the direction parallel to the emission plane were put on y-axis. From the projected spectra, the number of perpendicular and parallel scatterings for a given gamma, could be obtained. A near zero value of PDCO is indicative of a mixed transition while a positive value corresponds to an electric transition and a negative value, to a magnetic transition [18].

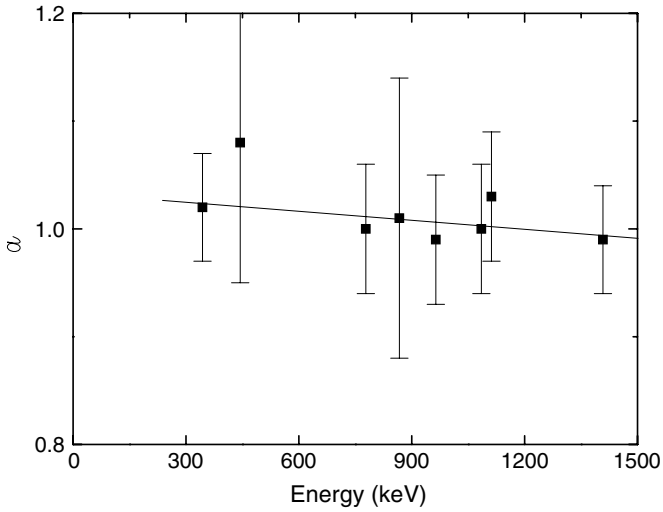

FIG. 1. Plot of correction factor (a) in PDCO measurement as a function of energy ($E\gamma$) for the clover detector array. The solid line shows the best χ^2 fit to the data points.

This method of evaluating the asymmetry is called the integrated PDCO [18]. However, since the experimental values of the PDCO were not corrected for the solid angle, not covered by the detectors, the asymmetry measured in the integrated mode can only be treated as qualitative information and may be used to rule out some transition modes for the γ-rays observed in the present experiment. The matrices were analysed using the codes RADWARE [19] and INGASORT [20].

IV. RESULTS

The partial level scheme of ^{143}Sm, shown in Fig. 2 (sequences I, II, III, IV), has been established using the coincidence relationship, relative intensities, $R_{\rm DCO}$ and PDCO ratios. The level scheme has been extended upto $E_x \sim 12$ MeV and a tentative spin of $57/2\hbar$. Decay from the 30 ms isomer via 208 keV, 182 keV, 1573 keV, and 755 keV transitions were also observed in the present experiment in the singles mode and absent in the γ-γ coincidence data. All transitions above 2795 keV $23/2^-$ reported in the earlier work by Kownacki *et al.* [16], have been observed in the present experiment. In addition to the transitions known from the earlier work [16], 56 new gamma transitions belonging to ^{143}Sm have been observed and placed in the decay scheme. Representative background subtracted gated spectra are shown in Fig. 3. The energies, relative intensities, $R_{\rm DCO}$, PDCO and the assigned spin-parity of the relevant levels, of ^{143}Sm are given in Table I. As far as the parity assignments are concerned, owing to the insufficient statistics in the PDCO matrices, it was impossible, to quantify

TABLE I. Energy (E_γ), relative intensities (I_γ), $R_{\rm DCO}$, PDCO, spin-parity of the associated levels and electromagnetic assignments of the gamma transitions of ^{143}Sm populated in ^{130}Te(^{20}Ne,7n) reaction. All the DCO ratios are in pure dipole ($M1$) gate.

$E\gamma$ (keV)	$I\gamma$[a]	E_i (keV)	J_i	J_f	$R_{\rm DCO}$	PDCO	Assignment
122		3723	$25/2^-$	$25/2^-$			
126		7517	$(39/2^-)$	$37/2^-$			
150	8(12)	5837	$35/2^-$	$33/2^-$	1.40(0.15)	−ve	$M1/E2$
167	99(2)	3890	$27/2^-$	$25/2^-$	1.00	−0.15(0.19)	$M1$
172	35(4)	5452	$31/2^+$	$31/2^+$	1.11(0.03)	−0.19(0.20)	$M1$
197		6958	$(37/2^+)$	$37/2^+$			
228	35(3)	5915	$35/2^+$	$33/2^+$	1.60(0.05)	−0.06(0.10)	$M1/E2$
235	68(2)	5687	$33/2^+$	$31/2^+$	1.00(0.17)	−0.12(0.11)	$M1$
239	17(6)	8852	$(45/2^-)$	$(43/2^-)$	1.00(0.14)	−0.23(0.33)	$M1$
243	14(7)	5897	$33/2^-$	$31/2^-$	1.25(0.15)	−0.01(0.02)	$M1$
243		7599	$(41/2^+)$	$(39/2^+)$	1.00(0.12)		$(M1)$
293	6(5)	7875	$(45/2^+)$	$(43/2^+)$			$(M1)$
307	92(2)	4197	$29/2^-$	$27/2^-$	1.31(0.03)	−0.04(0.11)	$M1/E2$
340	18(12)	9192	$(47/2^-)$	$(45/2^-)$	1.00(0.04)	−0.17(0.15)	$M1$
364	14(12)	7391	$37/2^-$	$35/2^-$	1.25(0.06)	−0.16(0.18)	$M1/E2$
366		4563		$29/2^-$			
383	12(40)	7582	$(43/2^+)$	$(39/2^+)$	2.00(0.36)	+ve	$(E2)$
397		6084		$33/2^+$			
414		8612	$(43/2^-)$	$(41/2^-)$			$(M1)$
433		7027	$35/2^-$	$(35/2^-)$			
444	12(16)	9636	$(49/2^-)$	$(47/2^-)$	1.00(0.08)		$M1$
469	13(14)	4360	$29/2^-$	$27/2^-$	1.25(0.13)	0.07(0.27)	$M1/E2$
489		8364	$(47/2^+)$	$(45/2^+)$			
493		7582	$43/2^+$				
574	7(17)	7199	$(39/2^+)$	$37/2^+$	1.60(0.19)		$(M1/E2)$
578	5(13)	10214	$(51/2^-)$	$(49/2^-)$	1.00(0.09)	−0.24(0.34)	$M1$
595	14(13)	7356	$(39/2^+)$	$37/2^+$	1.25(0.64)	−0.18(0.22)	$(M1/E2)$
602	4(19)	10816	$(53/2^-)$	$(51/2^-)$	1.00(0.20)		$M1$
678		4649	$27/2^-$	$25/2^-$			$(M1)$
681		8198	$(41/2^-)$	$(39/2^-)$		−ve	$(M1)$
706	2(14)	12249	$(57/2^-)$	$(55/2^-)$			$(M1)$
710	5(20)	6625	$37/2^+$	$35/2^+$	1.33(0.12)	−0.22(0.24)	$M1$
727	2(7)	11543	$(55/2^-)$	$(53/2^-)$	1.00(0.35)	−ve	$M1$
797	6(19)	6712	$39/2^+$	$35/2^+$			$(E2)$
806	36(3)	3601	$25/2^-$	$23/2^-$	0.93(0.06)	−0.15(0.10)	$M1$
846	12(5)	6761	$37/2^+$	$35/2^+$	1.50(0.30)	−0.14(0.21)	$M1/E2$
863		6761	$37/2^+$	$33/2^-$			$(M2)$
875	17(4)	6712	$39/2^-$	$35/2^-$	1.50(0.17)	0.32(0.27)	$E2$
920	19(6)	5280	$31/2^+$	$29/2^-$	1.57(0.13)	0.13(0.23)	$E1$
926	15(23)	4649	$27/2^-$	$25/2^-$			$(M1)$
928	100	3723	$25/2^-$	$23/2^-$	1.33(0.03)	−0.03(0.06)	$M1/E2$
940		6594	$(35/2^-)$	$31/2^-$			$(E2)$
944		7027	$35/2^-$				
961		4562		$25/2^-$		−0.26(0.29)	
1005	19(8)	5654	$31/2^-$	$27/2^-$	1.5(0.45)	0.27(0.22)	$E2$
1014	11(7)	8613	$(43/2^-)$	$(41/2^+)$	1.40(0.50)	0.28(0.19)	$E1$
1043	9(6)	6958	$(37/2^+)$	$35/2^+$			$(M1)$
1075		6762	$37/2^+$	$33/2^+$			$(E2)$
1083	35(5)	5280	$31/2^+$	$29/2^-$	1.38(0.05)	0.11(0.13)	$E1$
1096	25(24)	8613	$(43/2^-)$	$(39/2^-)$	1.33(0.55)	0.17(0.08)	$E2$
1130	12(6)	7027	$35/2^-$	$33/2^-$	1.33(0.55)	−0.08(0.18)	$M1/E2$
1174		7089		$35/2^+$			
1176	22(3)	3971	$25/2^-$	$23/2^-$		−ve	$(M1)$
1255	35(6)	5452	$31/2^+$	$29/2^-$	1.06(0.06)	0.16(0.09)	$E1$
1854		4649	$27/2^-$	$23/2^-$			$(E2)$

[a]The quoted errors in the intensity include errors due to background subtraction, peak fitting and efficiency correction.

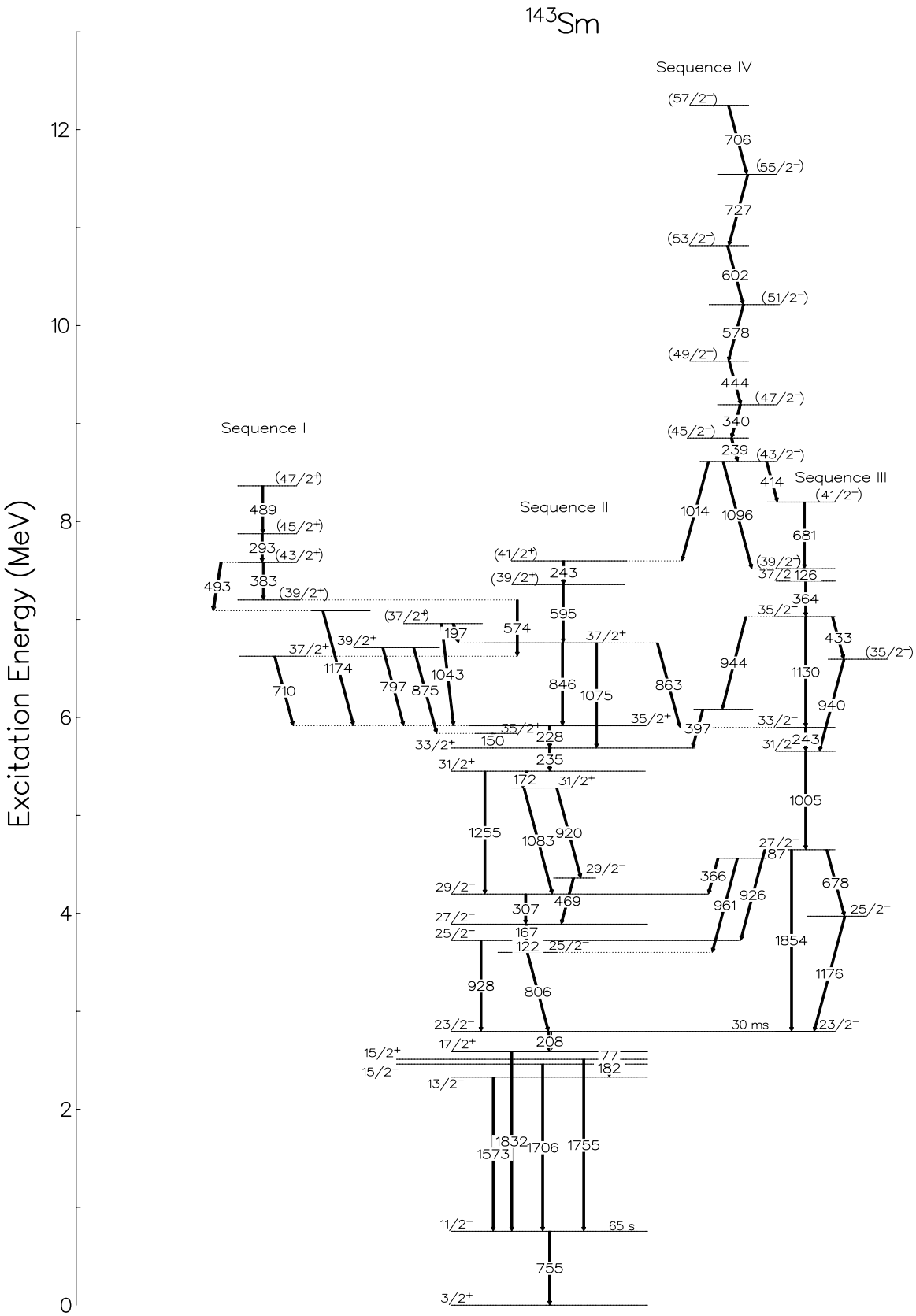

FIG. 2. Level scheme of ^{143}Sm. Levels and corresponding transitions below the 30 ms isomer are from Ref. [16].

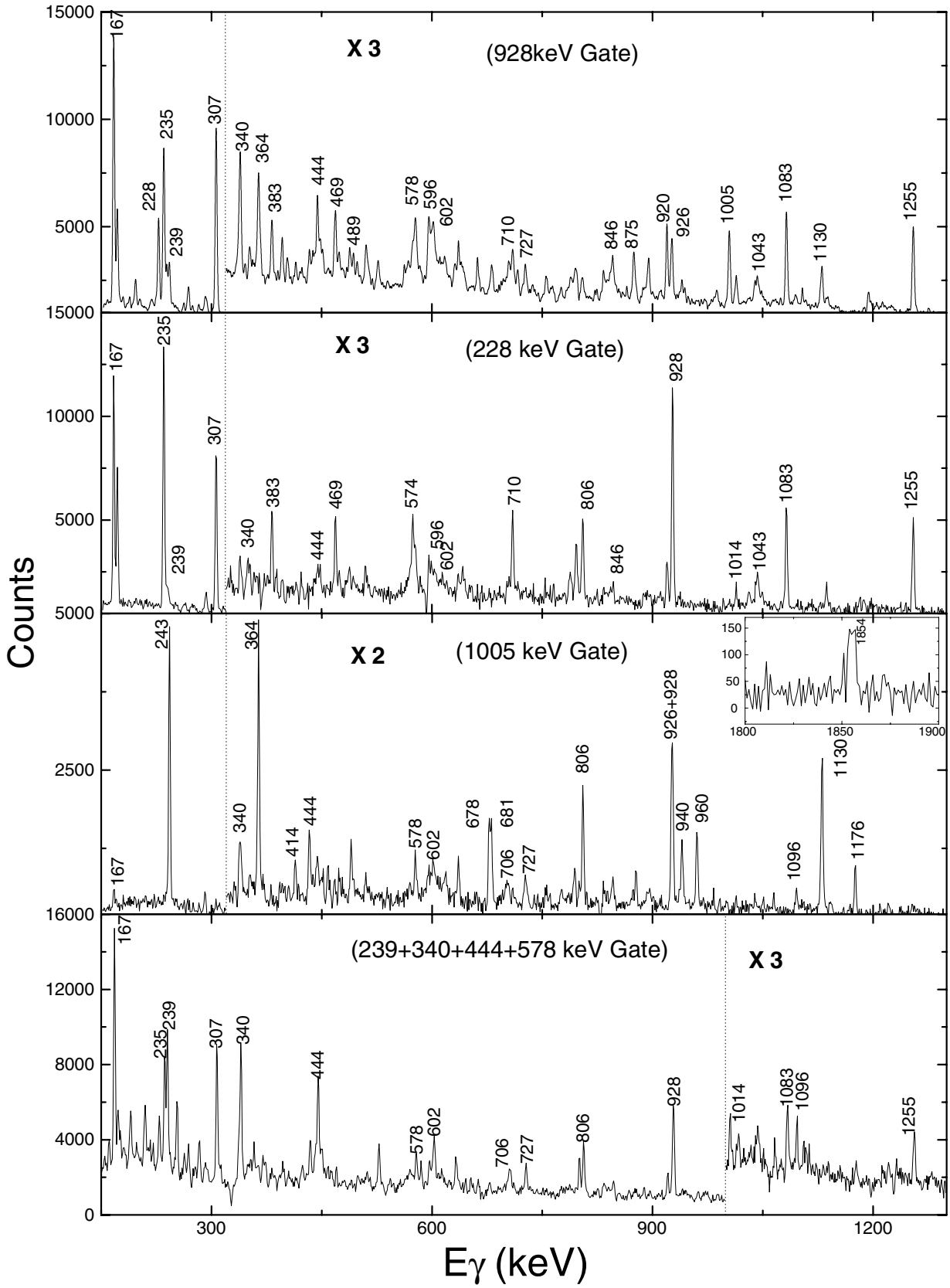

FIG. 3. Representative γ-γ coincidence spectra with various gates on transitions belonging to sequences I, II, and III. The inset to 1005 keV gated spectrum shows the 1854 keV transition.

the PDCO ratio for some transitions. However, it was often possible to state qualitatively, whether the ratio is positive or negative. Those have been indicated in the Table I. As a reference, the PDCO of the well established $M1$ transition, 389 keV of ^{143}Pm [21], populated in the present experiment, have also been calculated, alongwith the observed transitions, in order to verify the consistency of the method of analysis. The results show negative value for the previously established $M1$ transition, in compliance with expectation.

To begin with sequence II, the 928 keV transition right above the 30 ms isomer, is found to be a composite peak, as opposed to the previous work [16], as elaborated later. Parallel to the 928 keV is the 806 keV transition deexciting the 3601 keV state. The 3601 keV state did not have a unique spin-parity assignment in the earlier reference [16]. In the present work, the R_{DCO} and the PDCO measurements of 806 keV transition establish it's $M1$ character, following which the 3601 keV state has been assigned a spin-parity of $25/2^-$. The 167 keV ($27/2^- \rightarrow 25/2^-$) transition, in cascade with the 928 keV γ-ray, was previously reported to be a pure dipole and the spin 27/2 was assigned to the state deexcited by the 167 keV transition, without any parity assignment. Based on the angular distribution data (at three angles 40°, 55° and 90°), and the polarization measurement within the purview of the present work, we have conclusively identified the 167 keV transition as an $M1$ transition. Having confirmed the pure dipole nature of 167 keV gamma, it was used as a gating transition in calculating the R_{DCO} for several other transitions. The 307 keV gamma, in cascade with the 167 keV transition, was also reported earlier [16] and a spin 29/2 was assigned to the state thus deexcited, from the angular distribution data. In our work we have obtained R_{DCO} and PDCO values as 1.31 and -0.04, respectively, for the 307 keV transition. The R_{DCO} value reflects its mixed character and the most probable value of the PDCO complies to the assigned $M1/E2$ character of the 307 keV gamma. In line with this assignment, we have adopted the spin-parity $29/2^-$ for the state deexcited by the 307 keV transition.

Several new transitions in this sequence viz., 1255, 1083, 469, 920, 235, 228 keV were observed in the present experiment, above the earlier reported cascade of 928, 167, 307 keV transitions. The DCO ratio and the polarization measurement of the 1255 keV transition indicate that it is a pure $E1$ transition. So the spin-parity of the state deexciting by the 1255 keV has been assigned as $31/2^+$. This assignment also requires that the 1083 keV transition must have an $E1$ or predominantly $E1$ character. And simultaneously it is also required that the 172 keV transition, in cascade with the 1083 keV transition, be of $M1$ character. The R_{DCO} and the PDCO values of 1083 keV and 172 keV transitions are indeed consistent with their respective $E1$ and $M1$ assignment. In cascade with the 1255 keV and 172 keV transitions, is the 235 keV gamma which is a pure $M1$ transition, following the R_{DCO} and PDCO measurments. The 228 keV transition, from the consideration of its R_{DCO} and PDCO values is interpreted as a nonstretched quadrupole transition. Above the 228 keV transition the level scheme is fragmented, illustrated by the intensity pattern. In cascade with the 228 keV transition, leading to the higher lying states of sequence II, are three transitions viz., 846 keV, 595 keV and 243 keV. The 846 keV transition has been assigned a mixed $M1/E2$ character, from the measured R_{DCO} and PDCO values. As far as the 595 keV transition is concerned, the large errors in both the R_{DCO} and PDCO values keep us from emphatic conclusions on its electromagnetic character. However, in view of the values obtained in the R_{DCO} and PDCO measurements, the 595 keV transition has been tentatively assigned a mixed $M1/E2$ character, and the state thus deexcited, a most probable spin-parity of $39/2^+$. Following this tentative assignment, the spin-parity of the state deexcited by 243 keV transition is also tentatively assigned a spin-parity of $41/2^+$.

Sequence I consists of 710, 574, 383, 293, and 489 keV transitions and the relevant states of this sequence are positive parity states. The transitions are predominantly $M1/E2$ in character. There are indications of some weak connecting transitions between the sequences I and II but being very weak, these connecting transitions, could not be uniquely placed in the present work.

Sequence III is entirely a new sequence decaying to the 30 ms isomer. The main decay path of this sequence is via the transitions 961 and 926 keV, which are in cascade with the 806 and 928 keV transitions, respectively. The 928 keV peak was found to be a composite peak arising out of the 926 keV and 928 keV γ-rays. This is in contradiction to the earlier work [16] where the peak was attributed to only the 928 keV transition. The sequence also feeds the isomer at 2795 keV directly by the cascade 678 and 1176 keV transitions and the corresponding crossover, 1854 keV transition, observed in the 1005 keV gate, consolidates the fact. The PDCO measurement of 1005 keV transition shows it to be electric in nature. The DCO ratio of 1.5, for this transition, evaluated in 806 keV ($M1$) gate, justifies its $E2$ assignment. So the spin-parity of the state deexcited by the 1005 keV transition is proposed to be $31/2^-$. The transitions 243 keV, 1130 keV, 364 keV, 126 keV are in cascade with the 1005 keV transition. The R_{DCO} measurement of the 243, 1130, and 364 keV transition shows them to be of $M1/E2$ character. The PDCO measurement of the three transitions commensurate with this proposed assignment. Based on these measurements the spin-parity of the states deexcited by the 243, 1130, and 364 keV transitions are proposed to be $33/2^-$, $35/2^-$, and $37/2^-$, respectively. Once again, large error in the R_{DCO} value of 126 keV transition keeps us from being conclusive on the spin-parity of the associated state and we adopt a tentative assignment therein.

Sequence IV feeds the sequence II by a 1014 keV $E1$ transition and sequence III by the 1096 keV $E2$ transition, respectively. The placement of the 1014 keV transition connecting sequence II and sequence IV is crucial in view of the parity change involved. The $E1$ character of 1014 is established from the R_{DCO} and (positive) PDCO values. The DCO and the polarization measurements on the transitions in sequence IV, viz., 239, 340, 444, 578, 602, 727, 706 keV, show them to be of $M1$ in nature. The placement of transitions is from gated spectra. No crossover $E2$ transitions have been observed in this band. The gamma lines of this sequence do not show any detectable line shape and hence no information about the lifetime of the states could be obtained in the present experiment. In spite of the reasonably

convincing electromagnetic assignment ($M1$) to the transitions in sequence IV, the spin-parity of the states in this sequence, have been assigned only tentatively. This is in consequence to the tentative spin-parity assignments to the higher lying states of sequence II and III, owing to reasons discussed earlier.

Some weak transitions viz., 190, 252, 337, 512, 527, 636, 755 keV, observed in the various gated spectra, and confirmed as belonging to ^{143}Sm but could not be placed in the level scheme, owing to their weak nature and also due to the presence of strong contamination from the neighboring channels populated in the same reaction.

V. DISCUSSIONS

The nucleus ^{143}Sm has 81 neutrons and 62 protons and is in the vicinity of the $N = 82$ shell closure. It is also known that the nucleus ^{146}Gd behaves as a doubly closed nucleus as $Z = 64$ acts as a semimagic number. The low-lying few energy levels are basically one quasiparticle states [16]. The lowest positive parity state with spin-parity value of $3/2^+$ is known to arise from the $\nu 2d_{3/2}$ single particle orbital. The lowest negative parity state is the $11/2^-$ state at 755 keV ($\tau_{1/2} = 65$ s). This state is considered to be a one neutron quasiparticle state with one hole in $\nu h_{11/2}$ orbit. The next few states can be considered to arise out of coupling of the last neutron hole and excitation of the proton core. The core, ^{144}Sm, exhibits states with spin-parity values 2^+ and 3^-, which are expected to arise out of admixture of two proton quasiparticle configurations and collective vibration [22]. The next higher states with spin-parity values 4^+ and 6^+ have been shown to arise mainly out of two proton quasiparticle configurations. Kownacki *et al.* [16] have used hole vibration weak coupling and intermediate coupling models to describe these states which lie below the isomeric $23/2^-$ state at 2.795 MeV in ^{143}Sm. They have concluded that the intermediate coupling model describes the experimental data better. Assuming the $Z = 64$ to be the core, the $23/2^-$ isomeric state at 2.79 MeV has been proposed to be a three quasiparticle state with one neutron hole in the $\nu h_{11/2}$ level and two proton holes, one in each of $\pi d_{5/2}$ and $\pi g_{7/2}$ levels [16]. One, however, must note that the calculation of Kownacki *et al.* [16] could not explain the isomeric nature of the state as the particle-core coupling calculation predict a state with spin-parity of $19/2^-$ below this state arising from the $4^+ \otimes 11/2^-$ configuration. They had to assume that the latter state lies actually above the isomer.

We have tried to estimate the energy of the states using a particle hole calculation in the relativistic mean field approach using the blocked BCS method. In this method, one starts with a relativistic Lagrangian describing nucleons interacting via exchange of mesons. The Euler-Lagrange equations of motion have been obtained under the usual approximations, viz. classical meson fields, no contribution from the Dirac sea, time reversal symmetry, etc. The equations have been solved by expanding in a deformed harmonic oscillator basis. The force used is NLSH [23] known for its ability to describe the nuclei throughout the periodic table, and particularly in nuclei close to the stability valley. For the pairing, we have taken the pairing gap equal to that of the neighboring even-even nucleus ^{142}Sm. The pairing gap has been calculated from the odd-even mass difference. To make the calculations simple we have not changed the gap parameter for odd nucleus and interactions between different configuration have been neglected. We normalize the total binding energy so that the calculated energy of the $11/2^-$ state agrees with the experiment. Recently, the Sm nuclei have been studied in this formalism by Ming *et al.* [24]. The lighter isotopes of Sm are predicted to be nearly spherical in agreement with our calculation.

The results for some of the possible configurations are given in Table II. For the three quasiparticle $23/2^-$ isomeric state, the neutron hole is in the $h_{11/2}$ single particle state and the two proton holes are in $d_{5/2}$ and $g_{7/2}$ states, all the three orbitals being deformation aligned. The calculated energy of the three quasiparticle isomeric state based on the above configuration comes out to be 2.82 MeV, a value very close to the experimental value of 2.79 MeV. We have also investigated the nature of the excited states lying above this isomer. These states are likely to originate from the breaking of one or more pairs in the proton sector or the elevation of the pair as a whole from a low energy orbital to a high energy orbital or an interplay of the two mechanisms. The observed states are distinctly separated into two branches which again meet at the $43/2^-$ state at an energy of 8.61 MeV.

The observed sequences II and III are proposed to be generated by the breaking of the proton pairs. Thus they

TABLE II. The calculated results for different states and the energies of the corresponding experimental states. As all the states involved are weakly deformed, the single particle configurations are written in L_J form.

Nature of the state	Configuration	J^π	β(Calc.)	Energy (MeV)	
				Calculated	Experimental
1qp	$\nu h_{11/2}^{-1}$	$\frac{11}{2}^-$	0.05	0.76[a]	0.76
3qp	$\nu h_{11/2}^{-1}\pi(g_{7/2}^{-1}d_{5/2}^{-1})_6$	$\frac{23}{2}^-$	0.06	2.82	2.79
7qp	$\nu h_{11/2}^{-1}\pi(g_{7/2}^{-2}d_{5/2}^{-2})_{10}\pi(h_{11/2}^{2})_{10}$	$\frac{43}{2}^{-b}$		8.23	8.61
5qp	$\nu h_{11/2}^{-1}\pi(g_{7/2}^{-2}d_{5/2}^{-1})_{17/2}\pi h_{11/2}^{1}$	$\frac{29}{2}^+$		4.93	

[a]Normalized.

[b]Assumed to contain a rotational contribution of $3\hbar$.

are expected to be five quasiparticle states. The energy gap of approximately 800 keV above the isomeric state corresponds to the pair breaking energy. The 1255 keV transition in sequence II and 1014 keV connecting transition between sequences II and IV are the two parity changing transitions observed in the present experiment. The most likely explanation to such behavior is that the parity change occurs when one proton is excited from the $\pi(d_{5/2}g_{7/2})$ orbital to the intruder $\pi h_{11/2}$ orbital. In the present approach it is possible to calculate approximately, neglecting the mixing of the different possible configurations, the energy of the lowest positive parity state based on such a configuration, where one proton is in the $h_{11/2}$ orbital. The lowest positive parity states are expected to be around 4.93 MeV and the observed level at 5.28 MeV may actually be a higher excited state. A possible explanation for sequence III is that it contains the excitation of a pair from $\pi(d_{5/2}g_{7/2})$ orbital to the $\pi h_{11/2}$ orbital, as enlisted in Table II. At a higher excitation energy, angular momentum is generated by the breaking of the proton pairs.

One would also like to know the role of neutron excitation across the $N = 82$ shell gap. However, owing to the large energy gap, calculated to be more than 6 MeV, these states are expected to lie at a very high excitation energy. Experimentally also, we do not find any large transition indicative of neutron core excitation.

Sequence IV is a sequence of transitions between states with spin-parity, tentatively assigned as, $43/2^-$ and $57/2^-$, having regular spacing. We propose this sequence to be a $M1$ band having a seven quasiparticle configuration, based on $43/2^-$ state at an energy of 8.61 MeV. There are four proton holes in the $Z = 64$ closed shell, all being in deformation aligned high Ω orbitals, combining to produce angular momentum $10\hbar$. This is aligned with the spin of the neutron in the deformation aligned orbital to produce a total angular momentum of $31/2\hbar$. The two proton particles are in the low Ω orbital and hence are rotation aligned. They combine to produce an angular momentum of $10\hbar$. This is perpendicular to the earlier total angular momentum of the deformation aligned particles and the total angular momentum of this configuration is $37/2\hbar$. This is close to the tentatively assigned bandhead spin of $43/2^-$. The difference ($3\hbar$) can be attributed to the contribution from the core. The excitation energy of this state is calculated to be 8.23 MeV. Herein, we refer to the magnetic rotational band observed in ^{142}Gd that has been attributed a similar configuration [12]. The contribution from the core to the total angular momentum of the $M1$ band in the Pb region is typically $2\hbar$. It has been suggested that the contribution in the mass 140 region is larger than the mass 190 region [13].

Similar $\Delta I = 1$ cascades have been observed in Tb isotopes, $^{143-146}$Tb [5–8] nuclei. In ^{143}Tb, this cascade has been confirmed as a magnetic rotational band. Sequence IV has been found at an excitation energy $\sim$8.5 MeV similar to that observed in ^{146}Tb [8]. The sequence decays through high energy gamma transitions 1014 and 1096 keV, similar to the nuclei ^{143,146}Tb. A number of $M1$ bands in the neighboring $^{142-144}$Gd [9,10], ^{141}Eu [25] have been identified as "shears band." Lifetime measurements for the regular dipole band in

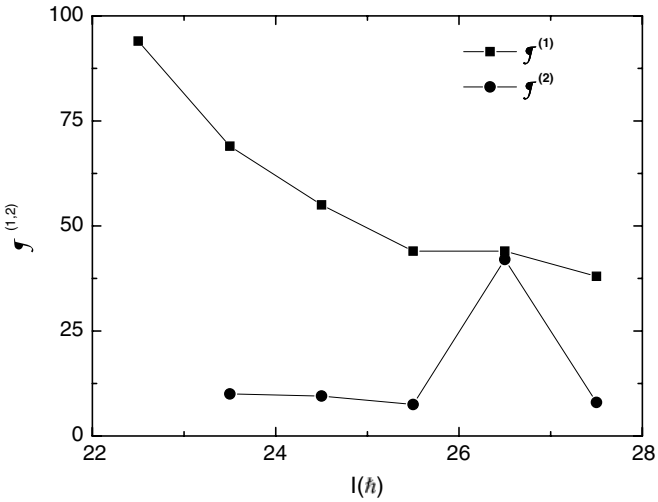

FIG. 4. Plot of kinetic ($\mathcal{J}^{(1)}$) and dynamic ($\mathcal{J}^{(2)}$) moment of inertia versus angular momentum (I) of the $M1$ sequence observed at $\sim$8.6 MeV in ^{143}Sm.

^{139}Sm [1] has shown it to be magnetic rotational band which was theoretically intepreted from TAC calculations to be of configuration $\nu h_{11/2} \otimes \pi h^2_{11/2}$. However, collective contribution to the angular momentim in ^{139}Sm [1] is somewhat higher compared to the Pb isotopes.

As pointed out earlier, sequence IV is proposed to be of the configuration $\pi[d^{-2}_{5/2}g^{-2}_{7/2}h^2_{11/2}] \otimes \nu h^{-1}_{11/2}$, at the excitation energy $\sim$8.5 MeV. It appears that this sequence is likely to be a magnetic rotational band observed in this region. This is also in conformity with the observation of Frauendorf [26] that weak deformation, and the existence of high j particles and high j holes, give rise to the formation of shears band in this mass region.

The kinetic moment of inertia, $\mathcal{J}^1 = \hbar I/\omega$ and dynamic moment of inertia $\mathcal{J}^2 = \hbar dI/d\omega$ are plotted against the spin I, in Fig. 4. The $\mathcal{J}^{(1)}$ value decreases with angular momentum I, as opposed to the normal rotational band that has $\mathcal{J}^{(1)}$ increasing with I. This reflects a large contribution to the total angular momentum from a source other than the collective motion. The small value of $\mathcal{J}^{(2)}$ is also indicative of large contribution to the total angular momentum from alignment. Calculation shows $\mathcal{J}^{(2)} \sim 10\hbar^2\,\mathrm{MeV}^{-1}$, smaller than that of normal rotational band. However, the sudden rise in the value of $\mathcal{J}^{(2)}$ at spin $51/2\hbar$ is not understood.

VI. CONCLUSIONS

The level scheme of ^{143}Sm has been extended upto $\sim$12 MeV of excitation energy and $\sim 57/2\hbar$ units of angular momentum. R_{DCO} and PDCO measurements have been made to assess the electromagnetic character of the transitions and to assign appropriate spin-parity to the observed levels, using special features of the Clover array. The possible configurations of the observed states have been discussed. At low energy the nucleus ^{143}Sm, as expected from shell model considerations, exhibits irregular excitation pattern. Theoretical calculations, using particle-hole configuration in the relativistic mean field

approach with blocked BCS method, have been made and were found to be satisfactory when compared with the experimental results. At higher excitation energy and angular momentum, a regular sequence of levels connected by $M1$ transitions has been observed. Considering its origin from the probable configurations and systematics observed in this mass region, this sequence of levels appear to be a magnetic rotational band. Further experimental information about the lifetime of the states in sequence IV for reliable determination of $B(M1)/B(E2)$ values would aid in the conclusive interpretation of the nature of this sequence. Such measurements are beyond the scope of the present work. Also, theoretical TAC calculations are required to confirm the shears character of the observed dipole band and have an understanding of the underlying microscopic configuration for the observed level structure.

ACKNOWLEDGMENTS

The authors would like to thank all the participants in the joint national effort to set up the INGA array at VECC, Kolkata. The help recieved from the accelarator staff and target lab at VECC is gratefully acknowledged.

[1] G. Hackman, S. M. Mullins, J. A. Kuehner, D. Prevost, J. C. Waddington, A. Galindo-Uribarri, V. P. Janzen, D. C. Radford, N. Schmeing, and D. Ward, Phys. Rev. C **47**, R433 (1993).

[2] D. S. Haslip, S. Flibotte, G. de France, M. Devlin, A. Galindo-Uribarri, G. Gervais, D. R. LaFosse, I. Y. Lee, F. Lerma, A. O. Macchiavelli, R. W. McLeod, S. M. Mullins, J. M. Nieminen, D. G. Sarantites, C. E. Svensson, J. C. Waddington, and J. N. Wilson, Phys. Rev. C **57**, 442 (1998).

[3] C. M. Petrache, G. Lo Bianco, D. Ward, A. Galindo-Uribarri, P. Spolaore, D. Bazzacco, T. Kroll, S. Lunardi, R. Menegazzo, C. Rossi Alvarez, A. O. Macchiavelli, M. Cromaz, P. Fallon, G. J. Lane, W. Gast, R. M. Lieder, G. Falconi, A. V. Afanasjev, and I. Ragnarsson, Phys. Rev. C **61**, 011305(R) (1999).

[4] F. Brandolini, M. Ionescu-Bujor, N. H. Medina, R. V. Ribas, D. Bazzacco, M. De Poli, P. Pavan, C. Rossi Alvarez, G. de Angelis, S. Lunardi, D. De Acuna, D. R. Napoli, and S. Frauendorf, Phys. Lett. **B388**, 468 (1996).

[5] Y. Zheng, X. H. Zhou, Y. H. Zhang, T. Hayakawa, M. Oshima, Y. Toh, T. Shizuma, J. Katakura, Y. Hatsukawa, M. Matsuda, H. Kusakari, M. Sugawara, K. Furuno, and T. Komatsubara, J. Phys. G **30**, 465 (2004).

[6] F. R. Espinoza-Quinones, M. A. Rizzutto, E. W. Cybulska, W. A. Seale, J. R. B. Oliveira, N. H. Medina, R. V. Ribas, M. N. Rao, D. Bazzacco, F. Brandolini, S. Lunardi, C. M. Petrache, Zs. Podolyak, C. Rossi-Alvarez, F. Soramel, C. A. Ur, M. A. Cardona, G. de Angelis, D. R. Napoli, P. Spolaore, A. Gadea, D. De Acuna, M. De Poli, E. Farnea, D. Foltescu, M. Ionescu-Bujor, A. Iordachescu, V. Roca, F. Terrasi, A. Chatterjee, A. Saxena, and L. Sajo Bohus, Phys. Rev. C **60**, 054304 (1999).

[7] M. Sferrazza, M. A. Cardona, D. Bazzacco, S. Lunardi, E. Maglione, and G. de Angelis, Z. Phys. A **354**, 157 (1996).

[8] Krishichayan, A. Chakraborty, S. S. Ghughre, R. Goswami, S. Mukhopadhyay, N. S. Pattabiraman, S. Ray, A. K. Sinha, S. Sarkar, P. V. Madhusudana Rao, U. Garg, S. K. Basu, B. K. Yogi, L. Chaturvedi, A. Dhal, R. K. Sinha, M. Saha Sarkar, S. Saha, R. Singh, R. K. Bhowmick, A. Jhingan, N. Madhavan, S. Muralithar, S. Nath, R. P. Singh, and P. Sugathan, Phys. Rev. C **70**, 044315 (2004).

[9] M. Sugawara, H. Kusakari, Y. Igari, M. Terui, K. Myojin, D. Nishimiya, S. Mitarai, M. Oshima, T. Hayakawa, M. Kidera, K. Furutaka, and Y. Hatsukawa, Z. Phys. A **358**, 1 (1997).

[10] T. Rzaca-Urban, S. Utzelmann, K. Strahle, R. M. Lieder, W. Gast, A. Georgiev, D. Kutchin, G. Marti, K. Spohr, P. von Brentano, J. Eberth, A. Dewald, J. Theuerkauf, I. Wiedenhofer, K. O. Zell, K. H. Maier, H. Grawe, J. Heese, H. Kluge, W. Urban, and R. Wyss, Nucl. Phys. **A579**, 319 (1994).

[11] C. M. Petrache, R. Venturelli, D. Vretenar, D. Bazzacco, G. Bonsignori, S. Brant, S. Lunardi, M. A. Rizzutto, C. Rossi Alvarez, G. de Angelis, M. De Poli, and D. R. Napoli, Nucl. Phys. **A617**, 228 (1997).

[12] R. M. Lieder, T. Rzaca-Urban, H. Brands, W. Gast, H. M Jager, L. Mihailescu, Z. Marcinkowska, W. Urban, T. Morek, Ch. Droste, P. Szymanski, S. Chmel, D. Bazzacco, G. Falconi, R. Menegazo, S. Lunardi, C. Rossi Alvarez, G. de Angelis, E. Farnea, A. Gadea, D. R. Napoli, Z. Podolyak, Ts. Venkova, and R. Wyss, Eur. Phys. J. A **13**, 297 (2002).

[13] H. Hubel, Prog. Part. Nucl. Phys. **54**, 1 (2005).

[14] S. Frauendorf, Nucl. Phys. **A557**, 259c (1993).

[15] W. Neubert, K. F. Alexander, H. Rotter, S. Chojnacki, Ch. Droste, J. Lewitowicz, and T. Morek, Nucl. Phys. **A131**, 225 (1969).

[16] J. Kowanacki, J. Ludziejewski, Z. Sujkowski, H. Arnold, and H. Ryde, Nucl. Phys. **A236**, 125 (1974).

[17] E. S. Macias, W. D. Ruther, D. C. Camp, and R. G. Lanier, Comput. Phys. Commun. **11**, 75 (1976).

[18] K. Starosta, T. Morek, Ch. Droste, S. G. Rohozinski, J. Srebrny, A. Wierzchucka, M. Bergstrom, B. Herskind, E. Melby, T. Czosnyka, and P. J. Napiorkowski, Nucl. Instrum. Methods Phys. Res. A **423**, 16 (1999).

[19] D. C. Radford, Nucl. Instrum. Methods Phys. Res. A **361**, 297 (1995).

[20] R. K. Bhowmick, INGASORT Manual, private communication (2003).

[21] Sarmishtha Bhattacharya, Somen Chanda, Dipa Bandyopadhyay, Swapan Kumar Basu, G. Mukherjee, S. Muralithar, R. P. Singh, R. K. Bhowmick, and S. S. Ghugre, Phys. Rev. C **62**, 024317 (2000).

[22] K. Heyde, M. Waroquier, and C. Vanden Berghe, Phys. Lett. **B35**, 211 (1971).

[23] M. M. Sharma, M. A. Nagarajan, and P. Ring, Phys. Lett. **B312**, 377 (1993).

[24] J. Meng, W. Zhang, S. G. Zhou, H. Toki, and L. S. Ceng, Eur. Phys. J. A **25**, 23 (2005).

[25] Z. Marcinkowska *et al*., Acta. Phys. Pol. B **34**, 2319 (2003).

[26] S. Frauendorf, Rev. Mod. Phys. **73**, 463 (2001).